The Bioscan AN INTERNATIONAL QUARTERLY JOURNAL OF LIFE SCIENCES 20(3): 1047-1062, 2025 www.thebioscan.com

Synthesis, Characterization, and In Silico Evaluation of Pyrazole-1,3,4-Oxadiazole Scaffolds as Aurora Kinase Inhibitors

Sampath Kumar[1], Jagadeshwar Vannada*

Department of Chemistry University College of Science, Osmania University, Hyderabad-500007, India.

Sampath Kumar: ousampath7@gmail.com

*Correspondence author Email: oujagan@gmail.com

DOI: https://doi.org/10.63001/tbs.2025.v20.i03.pp1048-1062

KEYWORDS

Pyrazole; 1,3,4-Oxadiazole; Aurora kinase A; Molecular docking; Anticancer agents; Kinase inhibitors; Medicinal chemistry; In silico studies.

Received on:
22-07-2025
Accepted on:
08-09-2025
Published on:
18-09-2025

Abstract

A robust and efficient synthetic strategy for a series of new pyrazole-linked 1,3,4-oxadiazole scaffolds was synthesized and structurally characterized 1H-NMR, 13C NMR, IR and ESI-MS. Comprehensive insilico studies were conducted to assess the inhibitory potential of all synthesized molecules towards aurora kinase, a critical regulator of cell cycle progression. Molecular docking of the synthesized derivatives revealed that molecules 4g and 4h exhibited superior Glide scores, glide energy, human oral absorption, comparable to clinically relevant aurora kinase inhibitor danusertib. Markedly, the conserved interaction with the key active site residues was consistently observed across the most active molecules and danusertib, underscoring its pivotal role in aurora kinase inhibition. Collectively, these findings highlight molecules 4g and 4h as promising lead molecules for further development as potent aurora kinase inhibitors with potential anti-cancer applications.

INTRODUCTION

Cancer remains a critical global health challenge, according to nearly 10 million deaths worldwide in 2020 and an estimated over 10.3 million deaths in 2025, with approximately 20 million new cases annually. The disease is characterized by uncontrolled cellular proliferation and metastatic spread, which underlie its lethality [1, 2]. Despite advances in early detection and treatment, the global cancer burden is projected to increase substantially without enhanced prevention and control strategies. New cancer diagnoses could reach over 30 million and deaths nearly 18-18.6 million by 2050, driven principally by population ageing, demographic growth and persistent exposure to risk factors [3]. Nearly half of all cancer deaths are now attributable to modifiable risk factors, including tobacco use, alcohol consumption, diet, obesity and environmental pollutants, highlighting the potential impact of targeted preventive interventions [4]. These projections underscore the urgent need for the discovery and development of new anticancer inhibitors with improved efficacy and safety profiles [5]. Five-membered heterocyclic compounds incorporating oxygen and nitrogen atoms were widely recognized as privileged scaffolds in medicinal chemistry, particularly for the development of anti-cancer agents [6]. Among these, pyrazole and 1,3,4-oxadiazole moieties have garnered significant attention due to their well-established pharmacological relevance. Clinically investigated molecules such as milciclib and Zibotentan exemplify the anticancer potential of these heterocycles [7, 8].

In addition to oncology, these motifs are also prevalent in compounds exhibiting antibiotic, antiretroviral and anti-inflammatory activities (Fig-1), highlighting their structural versatilly. Inspired by these observations, the present study focuses on the design and synthesis of new pyrazole linked 1,3,4-oxadiazole moieties to explore their anticancer potential through *insilico* molecular docking studies [9, 10]. In silico studies revealed that all synthesized compounds have shown good Human oral absorption, while several derivatives exhibited strong binding affinities, as evidenced by Glide scores and Glide energies [11]. Importantly, these compounds showed comparable binding parameters relative to the clinically used anticancer drug Danusertib [12].

1.1 Importance of the Pyrazole Moiety

Pyrazoles were a major family of five-membered heterocyclic aromatic organic moieties with two nitrogen atoms in the ring. The methods for its synthesis have been thoroughly researched and such research efforts have been prompted by various prospective uses, particularly in the scenario of severely substituted pyrazole derivatives [7]. Pyrazoles (Figure 1) contain Miliciclib (anticancer) [8], razaxaban (anticoagulants) [9], rimonabant (anti-obesity) [10] and mepirizole (anti-inflammatory) [11].

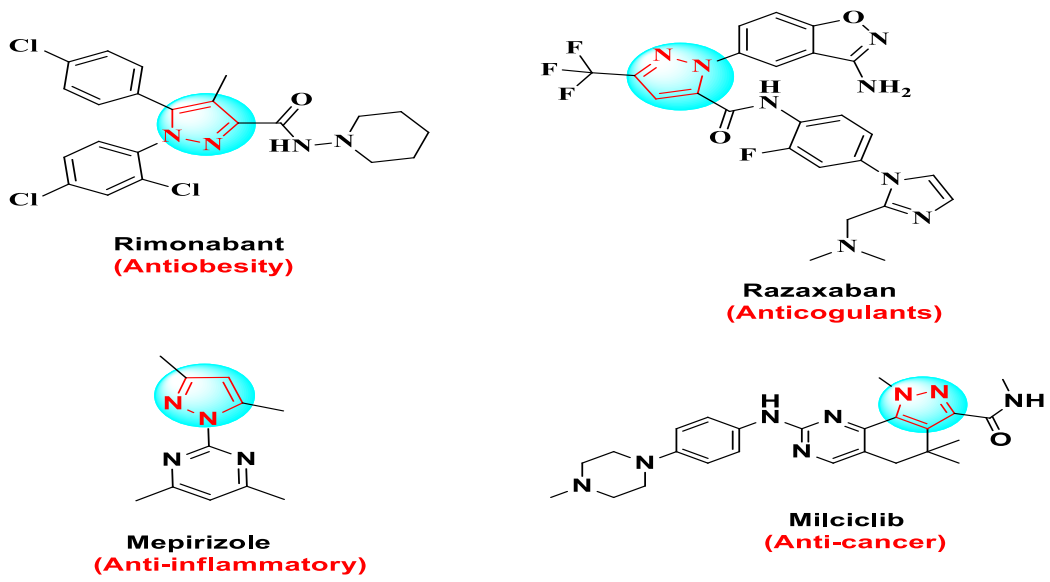

Figure 1: Biologically active drugs that consist of pyrazole

1 EXPERIMENTAL SECTION

All chemicals and reagents were of commercially available reagent grade and were used without further purification. Melting points were measured using a Veego melting point apparatus and are uncorrected. ^{1}H-NMR spectra were recorded on a Bruker AC-400F spectrometer Operating at 400MHz using $CDCl_3$ or deuterated DMSO as solvents, with chemical shifts reported in parts per million (ppm) relative to tetramethyl silane (TMS) as the internal standard. Reaction progress was monitored by thin-layer chromatography (TLC) on pre-coated silica gel 60 F_{254} plates (E. Merck, Germany) and spots wer visualized under UV light using a UV chamber (Perfit, India). Anhydrous sodium sulfate was employed as the drying agent.

1.1 General procedure of 1,3-diaryl-1H-pyrazole-4-carbohydrazide synthesis

1,1'- carbonyldiimidazole (CDI) (1.5mmol) and 1,3-diaryl-1H-pyrazole-4-carboxylic acid (1) (1.0mmol) were combined in dry THF and stirred for 2hours at room temperature. The reaction was monitored by TLC and then the solvent was evaporated under reduced pressure. The residue was refluxed with hydrazine hydrate (25mmol) in ethanol (10mL) for 10-12 hrs after the solvent was evaporated under low pressure and crude products were triturated with water. The precipitated solid was filtered and recrystallized from ethanol to get as white crystals [13].

1.2 General procedure of 2-(1,3-diaryl-1H-pyrazol-4-yl)-5-aryl-1,3,4-oxadizole synthesis:

Aromatic aldehyde (1.0 mmol) was added to the solution of acyl hydrazine (1.0mmol) in ethanol (10mL) and reaction mixture was reflux for 3-4 hrs. After completion of reaction (TLC), solvent was evaporated under reduced pressure and the resulting residue was redissolved in DMSO (5mL), followed by addition of potassium carbonate (3 mmol), iodine (1.2mmol) in sequence. The reaction mixture was stirred at 100 ºC until the conversion was completed for 1-4hrs (monitored by TLC). Following room temperature cooling, it was treated with 15 mL of 5% $Na_2S_2O_3$ and extracted using 10mL ×3 of ethyl acetate. The combined organic layers, washed with brine 10mL×1 and drying over anhydrous sodium sulphate. The given residue was purified through silica gel column chromatography with an eluent mixture of ethyl acetate and hexane [14]

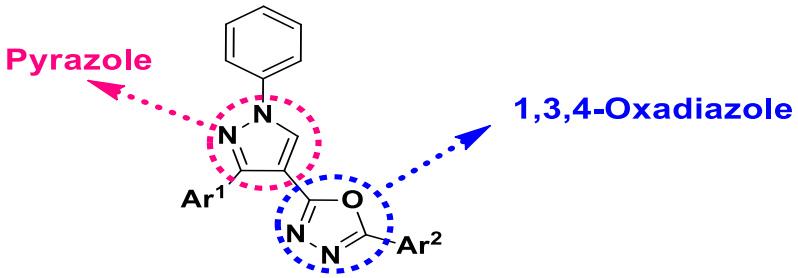

Figure2: Molecular structure of pyrazole-linked 1,3,4- oxadiazole derivative

1.3 Results and discussion

The synthesis of pyrazole linked 1,3,4-oxadiazole derivatives was carried out through a two-step route, as illustrated scheme 1. In the initial step, 1,3-substituted 1H-pyrazole -4- carboxylic acid was activated with CDI in dry THF at room temperature, followed by reaction with hydrate in ethanol under reflux to afford the corresponding acyl hydrazide (2a-d). Condensation of acyl hydrazide (2a-d) with aryl aldehydes (3a-c) in ethanol under reflux, followed by oxidative cyclization using iodine and potassium carbonate in DMSO, furnished the desired pyrazole linked 1,3,4-oxadizole derivatives(4a-l).

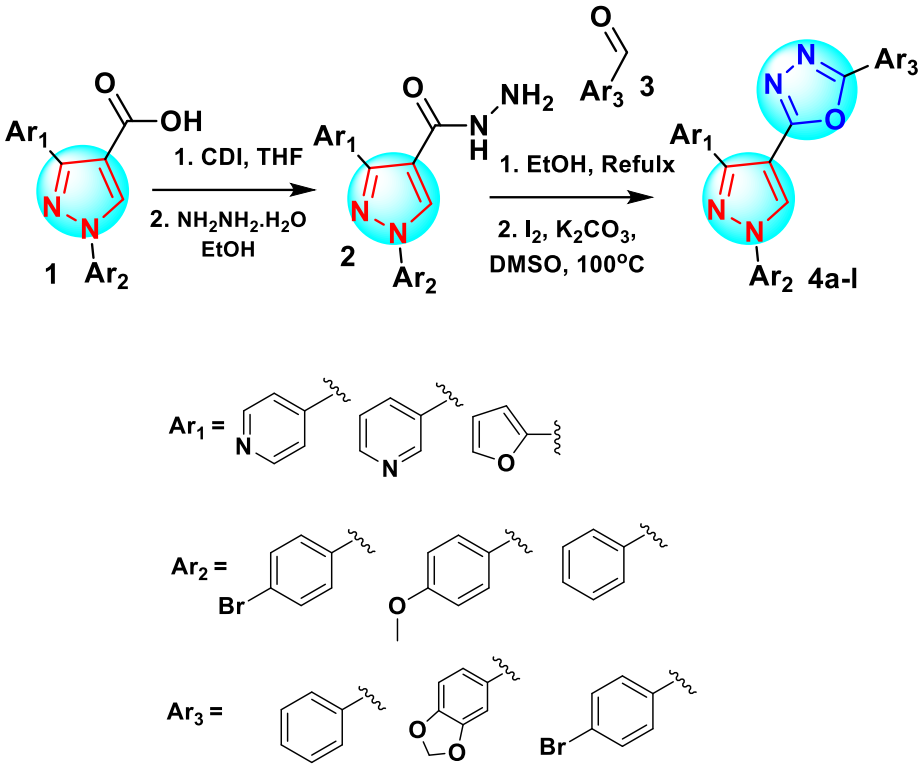

Figure3: Synthetic route for pyrazole -linked 1,3,4-oxadiazole derivatives(4a-l)

2 MOLECULAR DOCKING STUDIES

Molecular docking studies were carried out using the Glide module in the Maestro Schrodinger suite (Schrodinger, LLC). The X-ray crystallographic structure of Aurora Kinase (AURKA; PDB ID: 5DOS) was retrieved from Protein Data Bank [15, 16]. Protein preparation was performed using the Protein Preparation Wizard, which included assignment of bond orders, addition of hydrogn atoms, optimization of hydrogen-bonding networks and energy minimization under the OPLS-2025 force field to relieve steric clashes and optimize protein geometry [17]. Receptor grid was generated around the active site of the AURKA protein using the Glide module. All synthesized compounds (4a-l) were sketched using the Maestro Build Panel, converted into three-dimensional structures and prepared using the LigPrep module. Ligand preparation included geometry optimization and generation of low-energy conformers [18]. Subsequently, all twelve synthesized molecules were docked into the active site of AURKA using Glide [19]. The resulting docked complexes were evaluated and prioritized based on Glide docking scores, Glide scores and human oral absorption [20].

Molecular docking results indicate that compounds 4g and 4h formed stable protein-ligand complexes within the active site of AURKA, optimal glide docking scores and high predicted human oral absorption. These ligands consistently established H-bond and hydrophobic interactions with the key residues Lys166, Leu169, Gly175, Leu178, Arg179, Val182, His201 and Val206, suggesting that these residues contribute to ligand binding and AURKA inhibition [21, 22].

Table 1. Dock score, glide energy, Human oral Absorption and interaction of the synthesized molecules (4a-4l) and reference drug Danusertib with amino acid residues of AURKA protein.

Compound ID	Dock score	Glide energy	Human oral Absorption, %	Interactive amino acid residues
4a	-6.58	-47.48	100	Lys166, Leu178, Arg179, Val182, His201, Val206
4b	-6.73	-50.04	100	Lys166, Arg179, Val182, His201, Val206
4c	-7.01	-52.32	100	Lys166, Leu169, Gly175, Arg179, Val182, Tyr199, His201, Val206
4d	-6.71	-49.87	100	Lys166, Arg179, Val182, His201, Val206
4e	-6.34	-45.14	100	Lys166, Gly175, Arg179, Val182, Tyr199, His201, Val206
4f	-6.45	-46.49	100	Lys166, Leu169, Gly175, Arg179, Val182, Tyr199, His201, Val206
4g	**-7.45**	**-61.49**	**100**	Lys166, Leu169, Gly175, Arg179, Val182, His201, Val206
4h	**-7.12**	**-55.64**	**100**	Lys166, Leu169, Gly175, Leu178, Arg179, Val182, His201, Val206
4i	-6.84	-50.16	100	Lys166, Glu170, Gly175, Arg179, Val182, Tyr199, His201, Val206
4j	-6.34	-45.14	100	Lys166, Gly175, His201, Val206
4k	-6.97	-51.74	100	Lys166, Leu169, Gly175, Leu178, Arg179, Val182, Val206
4l	-6.64	-48.78	100	Lys166, Leu169, Gly175, Arg179, Val182, Val206
Danusertib	**-6.54**	**-45.87**	**92**	Lys166, Gly170, Arg179, Val182, Tyr199, His201, Ala203, Val206

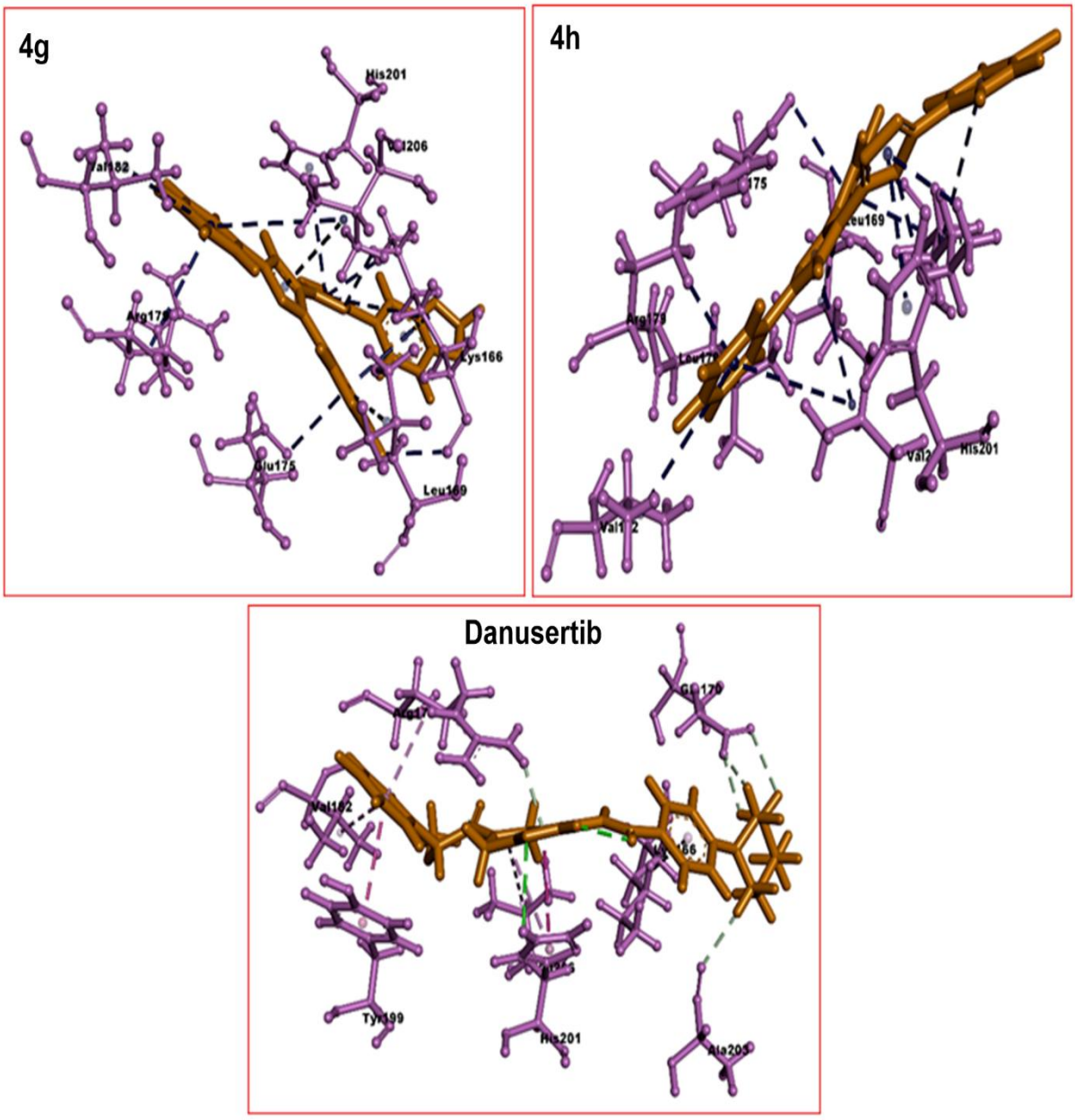

Fig. 2. The 4g, 4h molecule, danusertib drug docked into the active site of AURKA protein is represented in 3D and 2Dimentional representation

3 SPECTRAL DATA

3.1 2-(1-(4-bromophenyl)-3-(pyridin-4-yl)-1H-pyrazol-4-yl)-5-phenyl-1,3,4-oxadiazole (4a). Yield 90%, light brown solid, 195-200°C, R_f 0.40. ^{1}H-NMR spectrum ($CDCl_3$, 400MHz), δ, ppm: 8.83 (2H, s, Ar-H), 8.70 (1H, s, pyrazole CH), 7.87-7.82 (6H, m, Ar-H), 7.66-7.64 (2H, d, J=8.4 Hz, Ar-H), 7.55 (2H, t, J=7.6 Hz, Ar-H), 7.42 (1H, t, J=7.3 Hz, Ar-H). ^{13}C-NMR spectrum (DMSO-d_6-$CDCl_3$,101 MHz), δ, ppm: 105.8, 119.3, 120.6, 123.1, 127.8, 129.7, 130.8, 131.2, 131.3, 138.9, 150.2, 160.7, 161.8. IR spectrum, ν, cm^{-1}: 1292, 1550, 1631. ESI-MS: m/z: 443.85 $[M+H]^+$.

3.2 2-(1-(4-methoxyphenyl)-3-(pyridin-4-yl)-1H-pyrazol-4-yl)-5-phenyl-1,3,4-oxadiazole (4b). Yield 87%, Brown solid, 192-196°C, R_f 0.35. ^{1}H-NMR spectrum ($CDCl_3$, 400MHz), δ, ppm: 3.90 (3H, s, OCH_3), 7.05-7.03 (2H, m, ArH), 7.40 (1H, t, J=7.4 Hz, ArH), 7.55-7.51 (2H, m ArH), 7.89-7.82 (6H, m, ArH), 8.70 (1H, s, pyrazole CH), 8.81-8.80 (2H, dd, J=4.5, 1.6 Hz ArH) ^{13}C-NMR spectrum ($CDCl_3$,101 MHz), δ, ppm: 55.4, 105.7, 113.7, 119.5, 120.2, 121.6, 124.0, 127.7, 129.7, 130.4, 130.9, 131.7, 134.9, 150.7, 160.4, 161.0, 162.0. IR spectrum, ν, cm^{-1}: 1294, 1552, 1629. ESI-MS: m/z: 396.05 $[M+H]^+$.

3.3 2-(benzo[d][1,3] dioxol-5-yl)-5-(1-phenyl-3-(pyridin-4-yl)-1H-pyrazol-4-yl)-1,3,4-oxadiazole (4c) Yield 89%, light brown solid, 190-194°C, R_f 0.40. ^{1}H-NMR spectrum ($CDCl_3$, 400MHz), δ, ppm: 6.06 (2H, s, OCH_2O), 6.96-6.94 (1H, d, J=7.6 Hz, ArH), 7.44 (3H, m, ArH), 7.54 (2H, t, J=7.9 Hz, ArH), 7.85 (2H, m, ArH), 7.87 (2H, d, J=6.4Hz, ArH), 8.69 (1H, s, pyrazole CH), 8.82 (2H, dd, J=4.6, 1.4 Hz ArH). ^{13}C-NMR spectrum (DMSO-d_6-$CDCl_3$,101 MHz), δ, ppm: 101.7, 105.9, 108.5, 109.5, 119.3, 120.4, 123.3, 124.8, 127.9, 130.1, 132.0, 134.4, 139.1,

147.7, 148.4, 150.7, 152.9, 160.3, 161.7. IR spectrum, ν, cm^{-1}: 1234, 1546, 1627.ESI-MS: m/z: 410.00 $[M+H]^+$.

3.4 2-(4-bromophenyl)-5-(1-phenyl-3-(pyridin-4-yl)-1H-pyrazol-4-yl)-1,3,4-oxadiazole (4d)

Yield 92%, light brown solid, 195-198°C, R_f 0.45. ^{1}H-NMR spectrum ($CDCl_3$, 400MHz), δ, ppm: 7.40 (1H, t, J=7.2 Hz, ArH), 7.45 (2H, t, J=7.5 Hz, Ar-H), 7.64 (2H, d, J=8.3 Hz, ArH), 7.88-7.82 (6H, m, ArH), 8.71 (1H, s, pyrazole CH), 8.82 (2H, s, ArH). ^{13}C-NMR spectrum (DMSO-d_6-$CDCl_3$,101 MHz), δ, ppm: 105.7, 119.3, 120.6, 123.1, 127.8, 129.7, 130.8, 131.2, 131.3, 138.9, 150.2, 160.7, 161.8. IR spectrum, ν, cm^{-1}: 1234, 1546, **1629. ESI-MS: m/z: 444.06 [M+H]+.**

3.5 2-(1-(4-bromophenyl)-3-(pyridin-3-yl)-1H-pyrazol-4-yl)-5-phenyl-1,3,4-oxadiazole (4e)

Yield 94%, thick brown solid, 195-200°C, R_f 0.35. ^{1}H-NMR spectrum ($CDCl_3$, 400MHz), δ, ppm: 7.42 (1H, t, J=7.3 Hz, ArH), 7.53-7.50 (1H, m, ArH), 7.56 (2H, t, J=7.8 Hz, ArH), 7.66-7.62 (2H, m, ArH), 7.83 (2H, dd, J=8.5, 1.1 Hz, ArH), 7.89-7.86 (2H, m, ArH), 8.32-8.30 (1H, m, ArH), 8.70 (1H, s, pyrazole CH), 8.78 (1H, dd, J=4.8, 1.6 Hz, ArH), 9.22 (1H, d, J=1.4 Hz, ArH). ^{13}C-NMR spectrum (DMSO-d_6-$CDCl_3$,101 MHz), δ, ppm: 106.0, 119.3, 124.4, 127.7, 129.8, 130.9, 131.4, 131.6, 134.4, 139.0, 147.4, 149.9, 152.3, 160.2, 161.6. IR spectrum, ν, cm^{-1}: 1228, 1546, 1627. ESI-MS: m/z: 443.90 $[M+H]^+$.

3.6 2-(1-(4-methoxyphenyl)-3-(pyridin-3-yl)-1H-pyrazol-4-yl)-5-phenyl-1,3,4-oxadiazole (4f)

Yield 90%, light brown solid, 193-198°C, R_f 0.40. ^{1}H-NMR spectrum ($CDCl_3$, 400MHz), δ, ppm: 3.89 (3H, s, OCH_3), 7.04-7.02 (2H, d, J=8 Hz, ArH), 7.39 (1H, t, J=7.3 Hz, ArH),7.53-7.47 (1H, m, ArH), 7.54 (2H, t, J=7.8Hz, ArH), 7.84-7.82 (2H, d, J=8.3 Hz, ArH), 7.90-7.87 (2H, m, ArH), 8.32 (1H, m, ArH), 8.69 (1H, s, pyrazole CH), 8.77 (1H, dd, J=4.6, 1.3 Hz, ArH), 9.19 (1H, d, J=1.5Hz, ArH). ^{13}C-NMR spectrum (126 MHz, $CDCl_3$), δ, ppm: 55.4, 105.8, 113.7, 119.4, 123.9, 127.6, 129.5, 129.7, 130.4, 134.1, 139.1, 147.6, 151.8, 152.1, 160.4, 160.6, 161.6. IR spectrum, ν, cm^{-1}: 1232, 1510, 1635. ESI-MS: m/z: 395.90 $[M+H]^+$.

3.7 2-(benzo[d][1,3] dioxol-5-yl)-5-(1-phenyl-3-(pyridin-3-yl)-1H-pyrazol-4-yl)-1,3,4-oxadiazole (4g)

Yield 87%, brown solid, 195-200°C, R_f 0.40. ^{1}H-NMR spectrum (400MHz, DMSO-d_6), δ, ppm: 6.08 (2H, s, OCH_2O), 6.95-6.93 (1H, d, J=8.0 Hz, ArH), 7.28 (1H, t, J=7.4 Hz, ArH), 7.43 (1H, dd, J=3.0, 1.7 Hz, ArH), 7.45 (1H, d, J=1.7 Hz, ArH), 7.47 (1H, m, ArH), 7.50 (2H, t, J=7.8 Hz ArH), 7.92-7.89 (2H, m, ArH), 8.36-8.35 (1H, m, ArH), 8.71 (1H, s, pyrazole CH), 8.82 (1H, dd, J=4.8, 1.6 Hz, ArH), 9.23 (1H, d, J=1.6 Hz, ArH), ^{13}C-NMR spectrum (101 MHz, DMSO-d_6), δ, ppm: 101.7, 105.9, 108.5, 109.5, 119.3, 120.4, 123.3, 124.8, 125.6, 127.9, 130.1, 132.0, 134.4, 139.1, 147.7, 148.4, 150.7, 152.9, 160.3, 161.7. IR spectrum, ν, cm^{-1}: 1253, 1546, 1627. ESI-MS: m/z: 409.95 $[M+H]^+$.

3.8 2-(4-bromophenyl)-5-(1-phenyl-3-(pyridin-3-yl)-1H-pyrazol-4-yl)-1,3,4-oxadiazole (4h)

Yield 90%, light brown solid, 202-205°C, R_f 0.35. ^{1}H-NMR spectrum (400MHz, $CDCl_3$), δ, ppm: 7.40 (1H, t, J=7.2 Hz, ArH), 7.49-7.45 (1H, m, ArH), 7.53 (2H, t, J=7.6 Hz, ArH), 7.65-7.61 (2H, m, ArH), 7.83-7.81 (2H, dd, J=8.4, 1.2 Hz, ArH), 7.88-7.85 (2H, m, ArH), 8.31-8.28 (1H, m, ArH), 8.68 (1H, s, pyrazole CH), 8.78-8.76 (1H, dd, J=4.7, 1.8 Hz, ArH), 9.21 (1H, d, J=1.3 Hz). ^{13}C-NMR spectrum (DMSO-d_6-$CDCl_3$,101 MHz), δ, ppm: 106.0, 119.3, 124.4, 127.7, 129.8, 130.9, 131.4, 131.6, 134.4, 139.0, 147.4, 149.9, 152.3, 160.2, 161.6. IR spectrum, ν, cm^{-1}: 1298, 1550, 1624. ESI-MS: m/z: 444.14 $[M+H]^+$.

3.9 2-(1-(4-bromophenyl)-3-(furan-3-yl)-1H-pyrazol-4-yl)-5-phenyl-1,3,4-oxadiazole (4i)

Yield 87%, brown solid, 192-196°C, R_f 0.45. ^{1}H-NMR spectrum (400MHz, $CDCl_3$), δ, ppm: 6.70-6.67 (1H, m, ArH), 7.04 (1H, dd, J=1.4, 0.6 Hz, ArH), 7.40 (1H, t, J=7.4 Hz, ArH), 7.53 (2H, t, J=7.8 Hz, ArH), 7.64-7.62 (2H, m, ArH), 7.81 (2H, dd, J=8.6, 1.1 Hz, ArH), 7.85 (2H, dd, J=8.5, 1.5 Hz, ArH), 8.08 (1H, dd, J=1.9, 0.7 Hz, ArH), 8.68 (1H, s, pyrazole CH). ^{13}C-NMR spectrum (101 MHz, $CDCl_3$), δ, ppm: 106.6, 113.0, 114.6, 114.8, 120.3, 125.0, 128.4, 130.4, 130.5, 131.2, 140.0, 140.3, 146.6, 152.6, 157.6, 160.3,161.2. IR spectrum, ν, cm^{-1}: 1294, 1552, 1629. ESI-MS: m/z: 432.99 $[M+H]^+$.

3.10 2-(3-(furan-2-yl)-1-(4-methoxyphenyl)-1H-pyrazol-4-yl)-5-phenyl-1,3,4-oxadiazole (4j)

Yield 88%, light brown solid, 195-200°C, R_f 0.40. ^{1}H-NMR spectrum (400MHz, $CDCl_3$), δ, ppm: 3.87 (2H,

s, OCH_3), 6.59 (1H, d, J=1.6 Hz, ArH), 7.03 (2H, m, ArH), 7.05 (1H, dd, J= 1.5, 0.6 Hz, ArH), 7.40 (1H, t, J=7.5 Hz, ArH), 7.55 (2H, t, J=7.8 Hz, ArH), 7.84 (2H, d, J=2 Hz, ArH), 7.86 (2H, dd, J=1.3, 0.6), 8.05 (1H, dd, J=1.8, 0.9 Hz, ArH), 8.70 (1H, s, pyrazole CH). ^{13}C-NMR spectrum (101 MHz, $CDCl_3$), δ, ppm: 55.4, 105.7, 112.1, 113.7, 113.9, 119.4, 124.1, 127.5, 129.5, 129.6, 130.3, 139.1, 139.4, 145.7, 151.7, 156.7, 156.7, 159.4, 160.3. IR spectrum, ν, cm^{-1}: 1244, 1548, 1631. ESI-MS: m/z: 385.00 $[M+H]^+$.

3.11 2-(benzo[d][1,3] dioxol-5-yl)-5-(3-(furan-2-yl)-1-phenyl-1H-pyrazol-4-yl)-1,3,4-oxadiazole (4k)

Yield 85%, brown solid, 193-199°C, R_f 0.40. ^{1}H-NMR spectrum (400MHz, $CDCl_3$), δ, ppm: 6.02 (2H, s, OCH_2O), 6.69-6.65 (1H, m, ArH), 6.95-6.93 (1H, d, J=7.6 Hz, ArH), 7.05 (1H, dd, J=1.5, 0.6 Hz, ArH), 7.40 (1H, t, J=7.3 Hz, ArH), 7.42 (1H, dd, J=3.2, 1.4 Hz, ArH), 7.45 (1H, d, J=1.6 Hz, ArH), 7.52 (2H, J=7.7 Hz, ArH), 7.85 (2H, dd, J=3.2, 1.6 Hz, ArH), 8.07 (1H, dd, J=1.7, 0.7 Hz, ArH), 8.68 (1H, s, pyrazole CH). ^{13}C-NMR spectrum (101 MHz, $CDCl_3$ - DMSO-d_6), δ, ppm: 101.4, 105.5, 106.0, 108.2, 109.3, 112.6, 114.3, 119.2, 123.1, 125.5, 127.5, 129.7, 130.9, 139.1, 139.2, 146.5, 147.5, 148.3, 150.8, 160.2, 161.8. IR spectrum, ν, cm^{-1}: 1228, 1546, 1627. ESI-MS: m/z: 398.95 $[M+H]^+$.

3.12 2-(4-bromophenyl)-5-(3-(furan-3-yl)-1-phenyl-1H-pyrazol-4-yl)-1,3,4-oxadiazole (4l)

Yield 90%, thick brown solid, 197-202°C, R_f 0.45. ^{1}H-NMR spectrum (400MHz, $CDCl_3$), δ, ppm: 6.70-6.66 (1H, m, ArH), 7.03-7.01 (1H, d, J=8 Hz, ArH), 7.40 (1H, t, J=7.4Hz, ArH), 7.53 (2H, t, J=7.8 Hz, ArH), 7.53-7.51 (2H, d, J=7.9 Hz, ArH), 7.82-7.81 (2H, d, J=4Hz, ArH), 7.88-7.87 (2H, d, J=4 Hz, ArH), 8.15-8.13 (1H, d, J=7.8 Hz, ArH), 8.78 (1H, s, pyrazole CH). ^{13}C-NMR spectrum (126 MHz, $CDCl_3$), δ, ppm: 160.3, 159.4, 156.7, 151.7, 145.7, 139.4, 139.1, 130.3, 129.6, 129.5, 127.5, 124.1, 119.4, 113.9, 113.7, 112.1, 105.7. IR spectrum, ν, cm^{-1}: 1234, 1546, 1627. ESI-MS: m/z: 433.05 $[M+H]^+$.

4 CONCLUSIONS

We have synthesized novel pyrazole-linked 1,3,4-oxadiazole scaffolds with high yields and characterized by ^{1}H-NMR, ^{13}C NMR, IR and ESI-MS. The synthesized molecules were docked into the active site of Aurora

Kinase A protein. The synthesized molecules bind affinity to the current drug Danusertib with the AURKC protein, as shown by dock score, glide energy, and Human oral absorption. The active residues Lys166, Leu169, Gly175, Leu178, Arg179, Val182, His201 and Val206 of the AURKA protein were consistently bound to synthesized molecules, indicating that they were crucial for the inhibition of the AURKC protein. The 4g molecule outperformed the standard drug danusertib in terms of dock score (-7.45 kcal/mol), glide energy (-61.49 kcal/mol), with 100% human oral absorption, indicating that this molecule has potential therapeutic value against the aurora kinase A protein.

REFERENCES

1. Siegel RL, Kratzer TB, Giaquinto AN, Sung H, Jemal A. Cancer statistics, 2025. CA Cancer J Clin. 2025 Jan-Feb;75(1):10-45. doi: 10.3322/caac.21871. Epub 2025 Jan 16. PMID: 39817679; PMCID: PMC11745215.
2. Sansbury BM, Blackman E, Primm KM, Zaidi SK, Sengupta R. AACR Cancer Progress Report 2025: Unifying Cancer Science and Medicine: A Continuum of Innovation for Impact. Clin Cancer Res. 2025 Oct 15;31(20):4239-4243. doi: 10.1158/1078-0432.CCR-25-3366. PMID: 40960415.
3. Bowie K. Cancer deaths expected to reach 18 million by 2050, major study forecasts. BMJ. 2025 Sep 25;390:r2022. doi: 10.1136/bmj.r2022. PMID: 40998458.
4. Anand P, Kunnumakkara AB, Sundaram C, Harikumar KB, Tharakan ST, Lai OS, Sung B, Aggarwal BB. Cancer is a preventable disease that requires major lifestyle changes. Pharm Res. 2008 Sep;25(9):2097-116. doi: 10.1007/s11095-008-9661-9. Epub 2008 Jul 15. Erratum in: Pharm Res. 2008 Sep;25(9):2200. Kunnumakara, Ajaikumar B [corrected to Kunnumakkara, Ajaikumar B]. PMID: 18626751; PMCID: PMC2515569.
5. Częścik U, Gryglas M, Szterk A, Flis S. Evolution or Revolution in Colorectal Cancer Treatment: Present and Future of New Therapeutic Options. A Narrative Review. Oncol Res. 2026 Jan 19;34(2):2. doi: 10.32604/or.2025.067449. PMID:

41613807; PMCID: PMC12848744.

6. Kumar A, Singh AK, Singh H, Vijayan V, Kumar D, Naik J, Thareja S, Yadav JP, Pathak P, Grishina M, Verma A, Khalilullah H, Jaremko M, Emwas AH, Kumar P. Nitrogen Containing Heterocycles as Anticancer Agents: A Medicinal Chemistry Perspective. Pharmaceuticals (Basel). 2023 Feb 14;16(2):299. doi: 10.3390/ph16020299. PMID: 37259442; PMCID: PMC9965678.
7. Serag MI, Tawfik SS, Badr SMI, Eisa HM. New oxadiazole and pyrazoline derivatives as anti-proliferative agents targeting EGFR-TK: design, synthesis, biological evaluation and molecular docking study. Sci Rep. 2024 Mar 5;14(1):5474. doi: 10.1038/s41598-024-55046-0. PMID: 38443456; PMCID: PMC10915170.
8. K R K, Hacholli VB, Gackowski M, Pisklak DM, Kumar A, Szeleszczuk Ł. The Pyrazole Scaffold in Anticancer Drug Discovery: A Review of Synthetic Approaches, Structure-Activity Relationships, and Target-Based Mechanism of Action. Int J Mol Sci. 2026 Apr 10;27(8):3403. doi: 10.3390/ijms27083403. PMID: 42074046; PMCID: PMC13116616.
9. K R K, Hacholli VB, Gackowski M, Pisklak DM, Kumar A, Szeleszczuk Ł. The Pyrazole Scaffold in Anticancer Drug Discovery: A Review of Synthetic Approaches, Structure-Activity Relationships, and Target-Based Mechanism of Action. Int J Mol Sci. 2026 Apr 10;27(8):3403. doi: 10.3390/ijms27083403. PMID: 42074046; PMCID: PMC13116616.
10. Stecoza CE, Nitulescu GM, Draghici C, Caproiu MT, Olaru OT, Bostan M, Mihaila M. Synthesis and Anticancer Evaluation of New 1,3,4-Oxadiazole Derivatives. Pharmaceuticals (Basel). 2021 May 6;14(5):438. doi: 10.3390/ph14050438. PMID: 34066442; PMCID: PMC8148175.
11. Bodun DS, Omoboyowa DA, Olofinlade VF, Ayodeji AO, Mauri A, Ogbodo UC, Balogun TA. In-silico-based lead optimization of hit compounds targeting mitotic kinesin Eg5 for cancer management. In Silico Pharmacol. 2025 Jan 7;13(1):9. doi: 10.1007/s40203-024-00300-6. PMID: 39780769; PMCID: PMC11703796.

12. Steeghs N, Mathijssen RH, Wessels JA, de Graan AJ, van der Straaten T, Mariani M, Laffranchi B, Comis S, de Jonge MJ, Gelderblom H, Guchelaar HJ. Influence of pharmacogenetic variability on the pharmacokinetics and toxicity of the aurora kinase inhibitor danusertib. Invest New Drugs. 2011 Oct;29(5):953-62. doi: 10.1007/s10637-010-9405-7. Epub 2010 Feb 25. PMID: 20182906; PMCID: PMC3160560.

13. Baucom KD, Jones SC, Roberts SW. 1,1'-Carbonyldiimidazole (CDI) Mediated Coupling and Cyclization To Generate [1,2,4]Triazolo[4,3-a]pyridines. Org Lett. 2016 Feb 5;18(3):560-3. doi: 10.1021/acs.orglett.5b03589. Epub 2016 Jan 25. PMID: 26808327.

14. Yu W, Huang G, Zhang Y, Liu H, Dong L, Yu X, Li Y, Chang J. I2-mediated oxidative C-O bond formation for the synthesis of 1,3,4-oxadiazoles from aldehydes and hydrazides. J Org Chem. 2013 Oct 18;78(20):10337-43. doi: 10.1021/jo401751h. Epub 2013 Oct 8. PMID: 24059837.

15. S. David, Goodsell, D. Luigi, J. M. Costanzo, B. P. Duarte, I. Hudson, Persikova, J. Segura,, C. Shao. RCSB Protein Data Bank: Enabling biomedical research and drug discovery. Protein Sci. 29 (2020) 52-65, https://doi.org/10.1002/pro.3730.

16. Target Protein Structure Download. www.rcsb.org/ (accessed Feb 10, 2018).

17. Sastry G M, Adzhigirey M, Day T, Annabhimoju R and Sherman W 2013 Protein and ligand preparation: parameters, protocols, and influence on virtual screening enrichments *J. Comput. Aided Mol. Des*. **27** 221

18. LigPrep, Version, 3.3 2016 Schrodinger, LLC, New York, NY

19. R. A. Friesner, J. L. Banks, R. B. Murphy, T. A. Halgren, J. J. Klicic, D. T. Mainz, M. P. Repasky, E. H. Knoll, M. Shelley, J. K. Perry, D. E. Shaw, P. Francis, Glide: a new approach for rapid, accurate docking and scoring. 1. Method and assessment of docking accuracy. *J. med. chem*. *47* (2004) 1739-1749, https://doi.org/10.1021/jm0306430.

20. Lanka G, Bathula R, Dasari M, Nakkala S, Bhargavi M, Somadi G and Potlapally S R 2019 Structure-based identification of potential

novel inhibitors targeting FAM3B (PANDER) causing type 2 diabetes mellitus through virtual screening *J. Recept. Signal Transduct. Res.***39** 253

21. Liu S, Zhou L H, Wang H Q and Yao Z B 2010 Superimposing the 27 crystal protein/inhibitor complexes of β-secretase to calculate the binding affinities by the linear interaction energy method. *Bioorg. Med. Chem. Lett*. **20** 6533
22. Kawatkar S, Wang H, Czerminski R and Joseph-McCarthy D 2009 Virtual fragment screening: an exploration of various docking and scoring protocols for fragments using Glide *J. Comput. Aided Mol. Des*. **23** 527